Polarons generated by laser pulses in doped $LiNbO_3$

P. Herth, D. Schaniel, and Th. Woike
Institut für Mineralogie, Universität zu Köln, Zülpicher Strasse 49b, 50674 Köln, Germany

T. Granzow
Institut für Mineralogie, Universität zu Köln, Zülpicher Strasse 49b, 50674 Köln, Germany
and Fachbereich Material- und Geowissenschaften, TU Darmstadt, Germany

M. Imlau and E. Krätzig
Fachbereich Physik, Universität Osnabrück, Germany
(Received 23 July 2004; revised manuscript received 3 January 2005; published 28 March 2005)

The temporal behavior of polarons generated by pulsed illumination of $LiNbO_3$ crystals doped with Fe, Fe+Ti, and Cu is examined by detecting the light-induced absorption α_{li} in a pump-probe experiment. The decay of the polarons is satisfactorily described by a stretched exponential function over a temporal range of six decades. This fact is attributed to the dependence of the polaron lifetime on the distance to the nearest deep traps or to the disorder in $LiNbO_3$. The dependence of the amplitude and dynamics of the light-induced absorption on the pump intensity are explained within the framework of these models. The wavelength dependence of α_{li} displays a maximum at about 740 nm, revealing the optical excitation of small bound Nb_{Li}^{4+} polarons. Temperature-dependent measurements in the range 293–473 K reveal an Arrhenius behavior with an activation energy of about $E_A = 0.38$ eV.

DOI: 10.1103/PhysRevB.71.125128 PACS number(s): 71.38.−k, 77.84.Dy

I. INTRODUCTION

Single crystals of doped lithium-niobate ($LiNbO_3$) have received much attention due to their suitability for a wide range of practical applications. Most notable is the possibility to record and fix volume phase holograms. Thus it is a promising candidate as storage medium for volume holographic data storage,[1–4] a technique which combines high storage densities with fast data access. This technique makes use of the fact that electrons can be excited from traps—such as doping ions in the crystal—into the conduction band by inhomogeneous illumination. Migration of these charge carriers results in a space-charge field, which is an exact representation of the light-intensity pattern. Due to the linear electro-optic effect, this space-charge field causes a modulation of the refractive index, which can be read out by homogeneous illumination with light of the corresponding wavelength. However, according to the Bragg condition the wavelength of the reading and recording light has to be equal. This causes a redistribution of the charge carriers during read-out, thus completely erasing the space charge field and the holographically stored data, respectively. In order to overcome this problem a thermal fixing procedure was introduced,[5–7] which requires controlled heating of the storage material to temperatures of about 150 °C and results in nonvolatile space-charge fields stable over very long time scales of about 10–20 years.[8,9] For technical applications, however, this procedure is cumbersome and time consuming. As promising alternative, a two-step recording process has been presented.[8,10] During the first step of this process, electrons are excited by illumination with green or blue light from deep into shallow traps, which are energetically closer to the conduction band. In a second step the electrons are excited from these shallow traps by red or infrared (IR) light into the conduction band where they are redistributed. A space-charge grating occurs when the charges fall back into the deep traps. In comparison to the common one-step recording process this grating obviously can not be influenced by the reading light—i.e., by red or IR light. Thus the hologram can be recorded and read out using the same wavelength without erasure during read-out, precluding the need for a fixing procedure. The stored electron pattern is stable due to the two step process, and the lifetime of the written hologram depends on the dark conductivity of the material used.[11] In iron- or copper-doped $LiNbO_3$, the filled or unfilled traps are $Fe^{2+/3+}$ or $Cu^{+/2+}$, respectively.[12] Both, Fe^{2+} and Cu^{+} have an optical absorption at about 480 nm.[13]

Intense homogeneous sensitizing light—e.g., a short, intense laser pulse of sufficiently low wavelength—transfers electrons from these deep traps to the intrinsic defect Nb_{Li}^{5+} (Nb^{5+} on a Li^{+} site), forming a small bound polaron Nb_{Li}^{4+} (Ref. 14) and leaving behind an empty deep trap Fe^{3+} or Cu^{2+}, respectively. The small polaron has a characteristic broad absorption band in the red and near IR spectral range. Holograms can now be written by exciting electrons from the Nb_{Li}^{4+} centers.[15] The sensitizing illumination is a necessary prerequisite for the writing of holograms in the red or IR spectral range.

At room temperature, small polarons are not stable in $LiNbO_3$. The electrons relax back into the deep traps on a short time scale.[16] The lifetime of the polarons increases if the system is cooled, allowing a determination of the polaronic absorption band with optical spectroscopy. For the bound polaron Nb_{Li}^{4+} a maximum of the absorption was measured at about 775 nm at a temperature of $T = 100$ K. The absorption is nearly zero at 1300 nm and longer wavelengths.[17] Recently the absorption bands of polarons were detected at room temperature after pulsed electron

beam excitation[18,19] and earlier after x-ray irradiation.[20] The Nb_{Li}^{4+} polaron showed an absorption maximum at 1.6 eV in accordance with the results of Schirmer *et al.*[17]

It is obvious that for holographic two-step recording the light-induced absorption band of the polarons has to be known very well, especially at room temperature in the spectral range of 600–1300 nm and in dependence on the doping material as well as of the doping concentration. Furthermore, knowledge about the temporal development of the occupation and the temporal decay of polaronic centers after exposure to intense laser pulses as a function of the pulse intensity is required for effective hologram recording.

In this article, we present measurements of the light-induced absorption α_{li} in crystals of $LiNbO_3$ grown with the congruently melting composition and various doping materials (Fe, Cu, Ti). The temporal evolution of α_{li} probed at different wavelengths in the visible and near-IR spectral range is examined for several pulse intensities, polarization directions of the pump and probe waves, and pump light wavelengths. We show that small bound Nb_{Li}^{4+}-polarons are created in all doped $LiNbO_3$ single crystals. The activation energy and frequency factor are determined by temperature-dependent measurements. The results are discussed in the frame of excitation and deexcitation processes of polarons, as already presented in our earlier paper.[16]

II. EXPERIMENTAL DETAILS

Single crystals of congruently melting $LiNbO_3$ doped with 0.1 mol % Fe (LNB:Fe), 0.1 mol % Fe + 0.04 mol % Ti (LNB:Fe:Ti), and 0.08 mol % Cu (LNB:Cu) were cut into platelets with dimensions of $x=10$ mm, $y=8$ mm ($x \| c$ axis), and a thickness of $z=2$ mm. Except for the temperature-dependent measurements all measurements were performed at room temperature, $T=(298\pm1)$K. To determine the concentration of the doping ions in the samples, the optical absorption was detected for ordinary and extraordinary light polarization in the wavelength range from 400 to 1600 nm using a double-beam spectrophotometer. The dopant concentration of the Cu-doped sample was in addition determined by instrumental neutron activation analysis (INAA). The samples were then fixed onto a temperature-controlled holder which allowed us to vary the temperature in the range of 290 and 450 K. The main experiment itself was of the pump and probe type: The sample was illuminated by a laser pulse of a frequency-doubled Nd-YAG laser impinging normal to the large *xy* face of the sample. The pump wavelength λ_p could be varied by means of an optical parametric oscillator. Unless otherwise noted, $\lambda_p=532$ nm was used since this wavelength allowed the highest pulse intensity in the visible spectral range. The laser pulse duration was characterized by a full width at half maximum of 2.5 ns and a 10% point at 5.4 ns. The pulse energy was varied between $E_p=0.4$ mJ and $E_p=210$ mJ, corresponding to intensities of $I_p=1$ MW/cm^2 and $I_p=570$ MW/cm^2, respectively. The pump beam had a spatially rectangular flat-top profile, allowing a homogeneous illumination of the sample.

The temporal buildup and decay of the polarons was measured by detecting the changes of the intensity of a weak probe beam transmitted through the sample. To cover a broad spectral range, solid-state, diode, and gas lasers with wavelengths of 594, 608, 612, 633, 635, 658, 670, 685, 760, 785, 808, 850, 920, 1064, and 1310 nm were used as probe beam. The intensity I_s of the probe beam was adjusted for each measurement to strike a balance between a sufficiently large signal-to-noise ratio and the danger of influencing the system by the probe light. Generally, I_s did not exceed 3 mW/cm^2. The dependence of the obtained results on I_s was checked; where necessary, the influence of the probe light on the lifetime was corrected by varying the intensity of the probe light and extrapolating to zero. Unless otherwise noted, all experiments were performed with ordinary polarization of the probe beam. The angle between pump and probe beam was 5°. The intensity $I_s(t)$ of the probe beam was monitored by Si or InGaAs photodiodes with a rise time of less then 0.2 ns. The diodes detecting the probe beam were fitted with a set of interference filters so that the pump pulse did not adulterate the measurement. The signal of both diodes was fed to a digital storage oscilloscope with a band width of 2 GHz, a sampling rate of 16 Gsamples/s, and a memory for 64 Msamples, so $I(t)$ could be detected for a duration of 20 ms with a temporal resolution of 0.5 ns. The recording was triggered by the pump pulse, marking $t=0$ s. From $I_s(t)$, the light-induced absorption $\alpha_{li}(t)$ is determined by $\alpha_{li}(t)=(1/d)\ln[I_s(0)/I_s(t)]$, where $d=2$ mm is the crystal thickness.

III. EXPERIMENTAL RESULTS

A. Absorption coefficients

Figure 1 shows the absorption coefficients α_o and α_e of the three samples for ordinarily and extraordinarily polarized light. The curves have been corrected for the sample reflectivity. For both LNB:Fe and LNB:Fe:Ti, α_o clearly shows the Fe-absorption band around 485 nm. The pronounced peak is due to the presence of Fe^{3+} centers,[21] which undergo a spin-forbidden transition. In the α_e curves, this feature merely shows up as a shoulder in the onset of the fundamental absorption. The increase of the absorption coefficient α by a factor of 2 at 400 nm for the double-doped sample LNB:Fe:Ti compared to LNB:Fe results from the presence of Ti. The absorption bands of Ti^{3+} lie at about 730 nm for α_e and at about 620 nm for α_o,[22,23] but no notable features of Ti^{3+} are observed.

The LNB:Cu sample shows significantly higher absorption values compared to both Fe-doped samples. The absorption band at around 1100 nm is attributed to Cu^{2+} centers. At smaller wavelengths, the absorption caused by Cu^+ ions at around 380 nm extends into the onset of the fundamental absorption. The actual concentration c of Fe^{2+}, Cu^+, and Cu^{2+} ions is determined according to Refs. 7, 12, 13, and 24 from α_o (477 nm) and α_o (1040 nm), respectively. Our measurement resulted in $c_{Fe^{2+}}=(5.5\pm1)\times10^{23}$ m^{-3} for LNB:Fe and $c_{Cu^{2+}}=(16\pm3)\times10^{24}$ m^{-3} and $c_{Cu^+}=(6\pm3)\times10^{24}$ m^{-3} for LNB:Cu. By INAA measurement we received values of $c_{Cu}=(17\pm1)\times10^{24}$ m^{-3}. The slight discrepancy between the INAA and the absorption data probably results from the er-

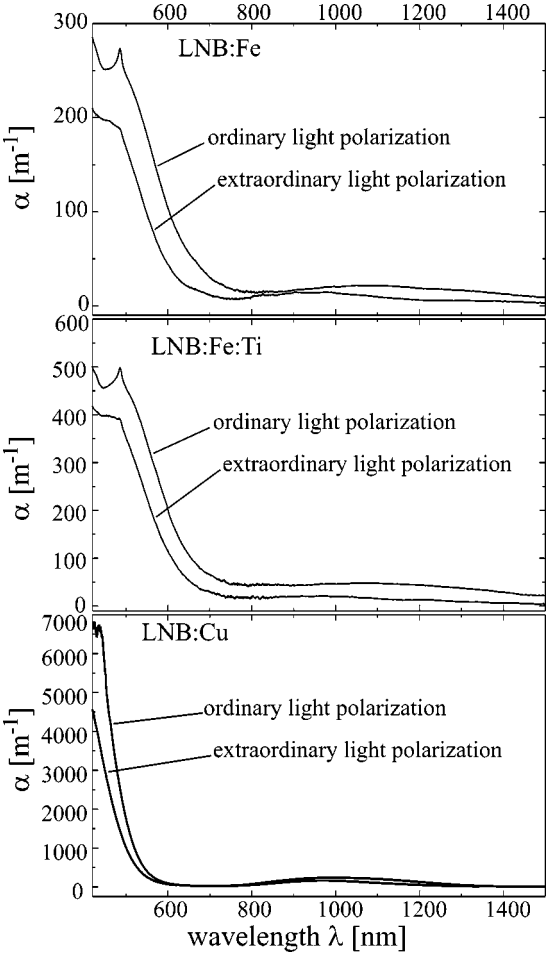

FIG. 1. Optical absorption α_o and α_e for ordinarily and extraordinarily polarized light of LNB:Fe, LNB:Fe:Ti, and LNB:Cu.

rors in the doping concentration of the samples used in Ref. 12. With our INAA measurements we present new reliable data for the Cu concentration in $LiNbO_3$. The extraction of the $c_{Fe^{2+}}$ concentration from the absorption spectrum of LNB:Fe:Ti has to be performed with caution. It is known that in the presence of titanium Fe ions are reduced,[25] resulting in an increase of $c_{Fe^{2+}}$ at a constant total concentration of Fe ions, $c_{Fe}=c_{Fe^{2+}}+c_{Fe^{3+}}$. If there is no contribution of Ti^{4+} to the absorption of the blue-green spectral range, an assumption justified by optical absorption measurements on $LiNbO_3$:Mg,Ti,[26] one obtains a concentration of $c_{Fe^{2+}}=(11\pm1)\times10^{23}$ m^{-3} for LNB:Fe:Ti. Consequently a significant higher α_{li} is expected as presented in Ref. 16.

B. Temporal evolution of α_{li}

Figure 2 exemplarily shows the temporal behavior of the light-induced absorption for LNB:Cu at $E_p=140$ mJ ($I_p=380$ MW/cm^2) with a probing wavelength of $\lambda_s=785$ nm. Under these conditions, α_{li} is about one order of magnitude larger than the basic optical absorption. In the inset, $\alpha_{li}(t)$ is depicted on a time scale of 3×10^{-10} s$\leqslant t\leqslant1\times10^{-8}$ s, together with the temporal behavior of the pump pulse. The

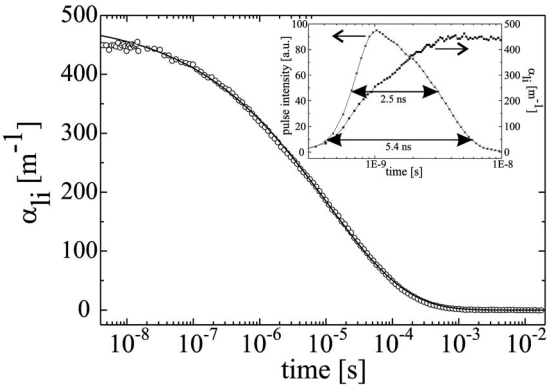

FIG. 2. Light-induced absorption $\alpha_{li}(t)$ in LNB:Cu for $E_p=140$ mJ, $\lambda_p=532$ nm, and $\lambda_s=785$ nm. The solid line represents a least-squares fit with Eq. (1). The inset shows the short-time behavior of α_{li} together with the pump pulse.

main part of Fig. 2 shows $\alpha_{li}(t)$ for 4×10^{-9} s$\leqslant t\leqslant2\times10^{-2}$ s. Note that the time axis has a logarithmic scale for both graphs in order to allow a better comparison of the short-time and long-time behavior of α_{li} over more then six orders of magnitude. The data points have been thinned out considerably to improve the clarity. During the first 3 ns, the buildup of α_{li} follows the increase of the intensity of the excitation pulse until the maximum of I_p is reached. There is no significant time lag between the exciting pulse and the resulting light-induced absorption. After the pulse has decreased to about 30% of its maximum, α_{li} starts to decay on a time scale of 1 ms. This temporal relaxation can be described very well with a stretched exponential function (KWW function) of the form

$$\alpha_{li}(t)=A_\alpha\exp[-(t/\tau)^\beta], \tag{1}$$

with the three parameters A_α, β, and τ. A least-squares fit of Eq. (1) to the measured data is represented by the solid line in Fig. 2. It obviously describes $\alpha_{li}(t)$ perfectly over more than six oders of magnitude in the time scale, resulting in values of $A_\alpha=493$ m^{-1}, $\tau=11$ μs, and $\beta=0.37$. Only at very short times $t<1\times10^{-8}$ s is there a small, but notable deviation of the fitted curve from the measured data points. At $t=5$ ns, the fitted values are 3% larger than the measured values. Extrapolation of the fitted $\alpha_{li}(t)$ curve to time scales below the duration of the laser pulse ($t<5$ ns) does not make physical sense. It should be noted in this context that the fitted value A_α does not characterize the magnitude of the light-induced absorption for very small time scales. In contrast to the assumption presented in Ref. 27, it is not directly correlated to the polaron density at $t=0$, and it is not identical to the observed maximum value α_{li}^{max}. Since the latter is a physically meaningful parameter, we will use it instead of A_α to quantify the size of the light-induced absorption.

The description of $\alpha_{li}(t)$ with a KWW function was possible for all samples using the entire range of pump intensities, probing wavelengths, light polarizations, and temperatures. We will therefore use the values of β and τ as measures for our further investigations of the light-induced absorption under the variation of the experimental condi-

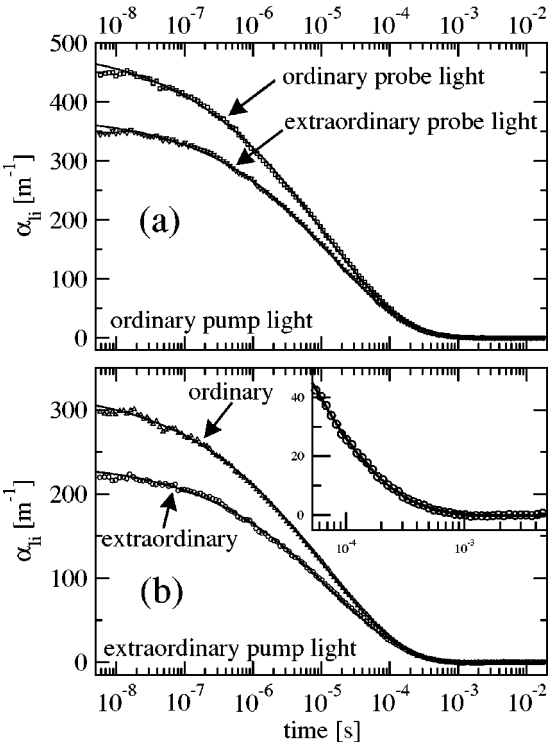

FIG. 3. $\alpha_{li}(t)$ of LNB:Cu for $E_p=140$ mJ, $\lambda_p=532$ nm, and $\lambda_s=785$ nm in dependence on the polarization of the pump and probe light. The inset illustrates the quality of the fit in the range 5×10^{-5}–5×10^{-3} s.

tions. First, we investigated the influence of the light polarization of the pump and probe light on the light-induced absorption. As an example the results are shown in Fig. 3 for LNB:Cu. The upper part (a) shows the curves obtained for both ordinarily and extraordinarily polarized probe light after excitation with an ordinarily polarized pump pulse. The lower part (b) shows the same for extraordinarily polarized pump light. The curves differ significantly in the values of α_{li}^{max}: While α_{li}^{max} reaches values of 450 m^{-1} for ordinarily polarized pump and probe light, it does not exceed 245 m^{-1} for extraordinary pump and probe light polarization. However, the dynamical behavior does not change, as it is reflected by the values of $\beta=0.38\pm0.02$ and $\tau=(1.0\pm0.1)\times10^{-5}$ s obtained from all four curves. The inset in Fig. 3(b) shows a magnification of the range 5×10^{-5}–5×10^{-3} s in order to demonstrate the quality of the fit with the stretched exponential function. Since the fundamental physical processes during the decay of polarons thus do not depend on the light polarization, we used only ordinarily polarized light in the following measurements to obtain large signals. The dependence of α_{li}^{max} on the polarization is found in accordance with results of electron beam excitation.[18]

In the next step the wavelength of the laser pulse λ_p was varied between 460 nm and 540 nm at a constant pulse energy of $E_p=5$ mJ ($I_p=13$ MW/cm^2) and $\lambda_s=785$ nm. These measurements showed an increase of α_{li}^{max} with decreasing λ_p, closely following the behavior of the optical absorption of the different samples. The decrease of β and τ by a factor of about 2 compared to the values observed using $E_p=140$ mJ ($I_p=380$ MW/cm^2) and $\lambda_p=532$ nm are explained by the lower pump intensity, as shown in the next chapter.

C. Intensity dependence of α_{li}^{max}, τ, and β

The measurements of $\alpha_{li}(t)$ indicate a strongly different behavior of the light-induced absorption with varying pump pulse energy. To investigate this influence of E_p systematically, measurements with $\lambda_p=532$ nm and $\lambda_s=785$ nm were performed with E_p varying in the range of $0.4\text{ mJ}\leqslant E_p\leqslant210$ mJ ($1\text{ MW/cm}^2\leqslant I_p\leqslant570\text{ MW/cm}^2$). As expected, α_{li}^{max} increased for all samples with increasing E_p. For a quantitative study, the energy of the incident pump pulse is not a suitable parameter: The pump light is partially reflected by the entrance and exit faces of each sample, and the light is absorbed inside the crystal. The incident pump intensity I_p is reduced to an effective pump intensity I_0, which is expressed by

$$I_0 = I_p \frac{4n e^{\alpha_o d}}{e^{\alpha_o d}(n+1)^2-(n-1)^2}\frac{1-e^{-\alpha_o d}}{\alpha_o d}, \tag{2}$$

where $n=2.33$ is the ordinary refractive index, α_o the absorption at $\lambda_p=532$ nm, and d is the sample thickness. The absorption α_{li}^{max} is plotted versus I_0 in part (a) of Fig. 4. If just two energetic levels are involved in the buildup, $\alpha_{li}^{max}(I_0)$ should follow an exponential function of the form

$$\alpha_{li}^{max}(I_0) = \alpha_{li,\infty}^{max}\left[1-\exp\left(-\frac{I_0}{I_\alpha}\right)\right], \tag{3}$$

with the saturation absorption $\alpha_{li,\infty}^{max}$ and the characteristic intensity I_α where 63% of $\alpha_{li,\infty}^{max}$ are reached. This function could be fitted satisfactorily to the measured data. Every point is measured twice. The results of the fit are represented by the solid lines in Fig. 4(a): the corresponding values are shown in Table I. At low pump intensities, the slope $d\alpha_{li}^{max}/dI_0$ should be proportional to the concentration c of the filled deep traps—i.e., Fe^{2+} and Cu^+, respectively: $d\alpha_{li}^{max}/dI_0=\kappa c$. Using the values of c obtained from the absorption measurements, we get $\kappa=(3.7\pm0.1)\times10^{-34}$ m^4/W for LNB:Fe, $\kappa=(2.0\pm0.2)\times10^{-34}$ m^4/W for LNB:Fe:Ti, and $\kappa=(8.9\pm0.1)\times10^{-35}$m^4/W for LNB:Cu. Here, we have used $c_{Fe^{2+}}=(11\pm1)\times10^{23}$ m^{-3} for LNB:Fe:Ti.

The temporal behavior of α_{li} was also influenced by changes in I_0: α_{li} was more persistent for higher pulse intensities. This qualitative observation is quantified by the results of the fits of Eq. (1) to the measured data. Parts (b) and (c) of Fig. 4 show $\beta(I_0)$ and $\tau(I_0)$, respectively. The values of β and τ increase strongly at low I_0 and reach saturation for the highest intensities. The solid lines are guides for the eyes. Two features are notable in this context: First, the light-induced absorption α_{li}^{max} is very similar for LNB:Fe and LNB:Fe:Ti, but the dynamics, characterized by β and τ, is not. The parameter β is larger by about 0.05 in LNB:Fe compared to LNB:Fe:Ti, and τ is reduced by a factor of 3 by codoping with Ti. Second, there appears to be a threshold behavior for the increase of τ in LNB:Cu: τ increases only very slightly (linearly) from 1×10^{-7} to 5×10^{-7} s until I_0 exceeds 25 MW/cm^2. Then it starts to rise drastically to sev-

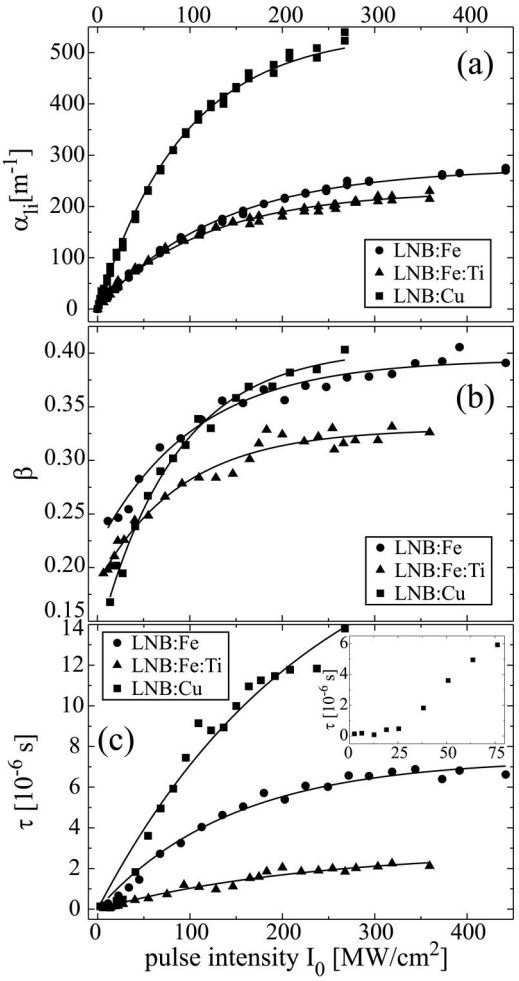

FIG. 4. Dependence of the light-induced absorption on the pump pulse intensity. Depicted are the maxima of the light-induced absorption $\alpha_{\mathrm{li}}^{\mathrm{max}}$ [part (a)] as well as the fitting parameters β [part (b)] and τ [part (c)]. The inset of part (c) shows a detailed view of the anomalous behavior of τ for LNB:Cu at low pump intensities.

eral μs. This behavior, which is not observed in the other two samples, is depicted in the inset of part (c) of Fig. 4. The quantities $\alpha_{\mathrm{li}}^{\mathrm{max}}$ and β do not show similar anomalies.

D. Wavelength dependence of $\alpha_{\mathrm{li}}^{\mathrm{max}}$

To determine whether other effects beside the formation of small bound Nb_{Li}^{4+} polarons play a role in building up the light-induced absorption, measurements of the dependence of α_{li} on the probing wavelength λ_s were performed at fixed values of E_p=150 mJ (I_p=400 MW/cm^2) and λ_p=532 nm.

TABLE I. Saturation absorption and characteristic pump intensity for the examined samples.

Sample	$\alpha_{\mathrm{li},\infty}^{\mathrm{max}}$ [m^{-1}]	I_α [MW/cm^2]
LNB:Fe	282±2	138±2
LNB:Fe:Ti	221±2	102±3
LNB:Cu	566±5	103±2

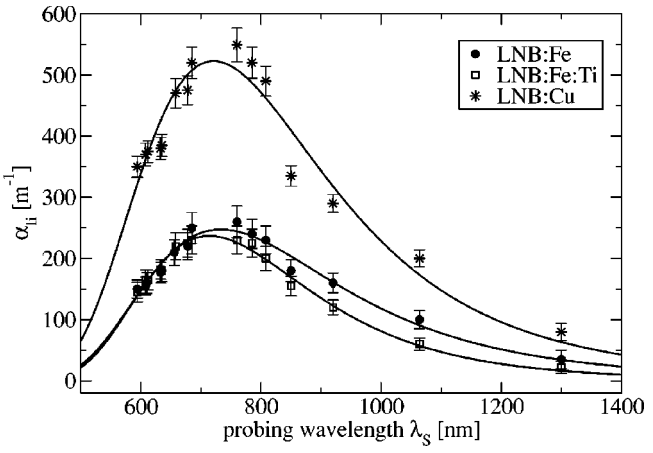

FIG. 5. Dependence of $\alpha_{\mathrm{li}}^{\mathrm{max}}$ on the wavelength of the probing beam. The solid lines represent fits of Eq. (4) to the measured data.

All $\alpha_{\mathrm{li}}(t)$ curves could be described with Eq. (1). The values of β and τ obtained from these fits for each sample were identical for all λ_s within the error margin. Notable changes were observed in the amplitude of the light induced absorption. Figure 5 shows the values of $\alpha_{\mathrm{li}}^{\mathrm{max}}$ obtained for the different probing wavelengths.

There is a notable $\alpha_{\mathrm{li}}^{\mathrm{max}}$ even at the shortest probing wavelength, λ_s=594 nm. For all samples, $\alpha_{\mathrm{li}}^{\mathrm{max}}$ first increases for increasing λ_s, peaks around 740 nm and then decreases. The absorption $\alpha_{\mathrm{li}}^{\mathrm{max}}$ does not reach zero even for λ_s=1300 nm. According to Refs. 17 and 28 the absorption band of the small bound Nb_{Li}^{4+} polarons can be described by a function of the form

$$\alpha_{\mathrm{li}}^{\mathrm{max}}(\omega) = D/\hbar\omega \exp\left(-\frac{(4U+\varepsilon-\hbar\omega)^2}{8U\hbar\omega_0}\right), \qquad (4)$$

where $\omega=2\pi c/\lambda_S$, $\hbar\omega_0$ is the representative phonon energy of the crystal, U is the polaron stabilization energy, and ε is the energy associated with the transfer of polarons between inequivalent sites. The constant D is a measure of the amplitude. The solid lines in Fig. 5 represent descriptions of the measured data with Eq. (4). Using the typical phonon energy $\hbar\omega_0 \approx 0.1$ eV, we obtain the stabilization energy U and the transfer energy ε. The fitted paramters are listed in Table II.

E. Temperature dependence and activation energy

It is important to know whether additionally free small polarons, having an absorption in the near-infrared spectral range, are generated by λ_p=532 nm. If the small deviation

TABLE II. Polaron stabilization energy U, transfer energy ε, and amplitude constant D.

Sample	U [eV]	ε [eV]	D [eV/m]
LNB:Cu	0.32±0.05	0.5±0.1	920±50
LNB:Fe	0.33±0.04	0.4±0.1	440±30
LNB:Fe:Ti	0.26±0.03	0.7±0.1	420±30

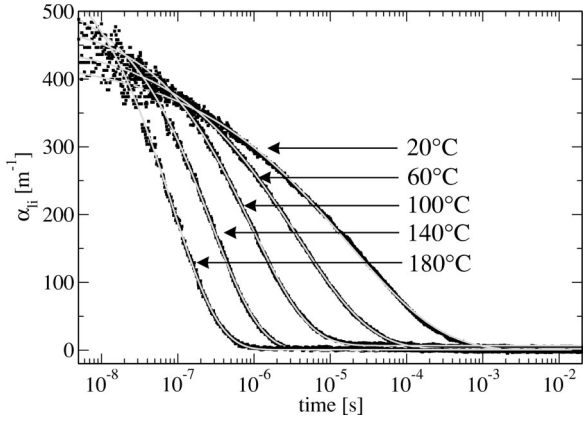

FIG. 6. The absorption $\alpha_{li}(t)$ of LNB:Cu at five different temperatures between 20 and 180 °C obtained for $E_p=140$ mJ, $\lambda_p=532$ nm, and $\lambda_s=785$ nm. The decay of the light-induced absorption accelerates with increasing temperature.

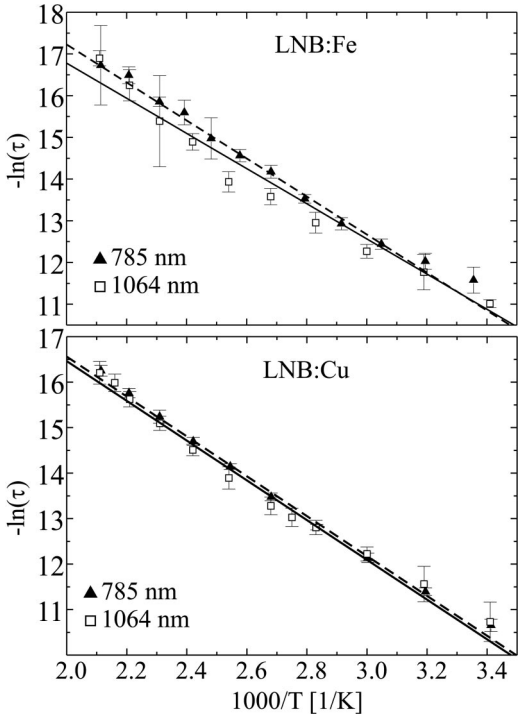

FIG. 7. Arrhenius plot of $-\ln(\tau)$ versus $1000/T$ for LNB:Fe and LNB:Cu. τ is obtained from a description of single $\alpha_{li}(t)$ curves with KWW functions. The straight lines are fits of Eq. (5) to the data obtained at $\lambda_s=785$ nm (dashed line) and $\lambda_s=1064$ nm (solid line).

from the fitted curves in Fig. 5 were due to a process besides the excitation of the Nb_{Li}^{4+} polaron, one can expect differences in the temperature behavior for the different probing wavelengths. We therefore have measured the temperature dependence of α_{li} for LNB:Fe and LNB:Cu at $E_p=150$ mJ ($I_p=400$ MW/cm^2) with two different probing wavelengths. The first, $\lambda_s=785$ nm, lies close to the maximum of the absorption band of the small bound Nb_{Li}^{4+} polaron. The second, $\lambda_s=1064$ nm, was chosen to detect the behavior of possibly created small free polarons.

Figure 6 exemplarily shows $\alpha_{li}(t)$ in LNB:Cu for five different temperatures T between 20 and 180 °C. As expected, the decay of the light-induced absorption is much faster if T is increased. α_{li}^{max} increases from 425 to 490 m^{-1} with increasing T. Quantitatively, the changes in the dynamics of the polaron decay are depicted in Fig. 7. It shows the logarithm of the time constant τ obtained from fitting Eq. (1) versus the reciprocal temperature for LNB:Fe [part (a)] and LNB:Cu [part (b)]. The scaling of the axes was chosen to check whether Arrhenius' equation

$$\tau^{-1} = Z \exp\left(-\frac{E_A}{k_B T}\right) \tag{5}$$

correctly describes the measured data, although we are aware of the fact that a distribution of lifetimes is involved in the decay processes. Here E_A is the activation energy which is necessary for the thermal decay of the polarons, Z is the attempt frequency, and k_B is Boltzmann's constant. As can be seen from the figure, Eq. (5) describes the measured data with reasonable accuracy. A least-squares fit, represented by the straight lines in Fig. 7, resulted in values of $E_A=(0.39\pm0.03)$ eV, $Z=(3\pm2)\times10^{11}$ Hz and $E_A=(0.36\pm0.03)$ eV, $Z=(9\pm6)\times10^{10}$ Hz, for LNB:Fe at $\lambda_s=785$ nm and $\lambda_s=1064$ nm, respectively. For LNB:Cu, $E_A=(0.38\pm0.03)$ eV, $Z=(10\pm4)\times10^{10}$ Hz and $E_A=(0.38\pm0.03)$ eV, $Z=(9\pm6)\times10^{10}$ Hz, respectively, was obtained for the two probing wavelengths. The stretching exponent β showed a general upward trend with increasing temperature, increasing from about 0.3 in the low-temperature limit to almost unity for the highest temperatures, in accordance with the results presented in Ref. 16.

IV. DISCUSSION

A. Temporal evolution of α_{li}

The completely reversible buildup of a light-induced absorption after illumination with an intense laser pulse can only be attributed to the formation of polarons: Electrons are excited from deep traps, in our case Cu^+ or Fe^{2+} ions, into their polaronic states. At a probing wavelength of 785 nm, our measurement is sensitive to the appearance of small bound Nb_{Li}^{4+} polarons at the most common crystal defect, a Nb atom on a Li lattice site. According to Ref. 15, the temporal change of the number of polarons N_X^- is described by the rate equation

$$\frac{\partial N_X^-}{\partial t} = -[\beta_X + q_X s_X I_s + \gamma_{XY}(N_Y - N_Y^-)]N_X^- + (\gamma_X n + q_{YX} s_{YX} I_p N_Y^-)(N_X - N_X^-). \tag{6}$$

Here β_X is the rate of thermal excitation of electrons from the Nb_{Li}^{4+} polarons into the conduction band and $q_X s_X$ is the cross section for absorption of probe-beam photons by Nb_{Li}^{4+} polarons and excitation of electrons into the conduction band. Similarly, $q_{YX} s_{YX}$ is the cross section for absorption of pump-beam photons by filled deep traps and excitation of electrons into Nb_{Li}^{4+} polarons. γ_X and γ_{XY} are the

coefficients for recombination of conduction band electrons with Nb^{5+} and electrons from Nb^{4+} with empty deep traps, respectively. N_Y and N_Y^- are the total number of deep traps and the number of filled deep traps, and N_X and N_X^- the number of Nb_{Li} atoms and Nb_{Li}^{4+} polarons, respectively. Furthermore, n is the number of conduction band electrons.

Since the buildup of the light-induced absorption is almost instantaneous, we can neglect the term $q_{YX}s_{YX}$ from Eq. (6) in the description of $\alpha_{li}(t)$ after the first 5 ns. The small deviation of less then 3% between the measured data and the curve according to Eq. (1) for 5 ns$<t<$10 ns seen in Fig. 2 can be attributed to the recombination of electrons raised by the pump pulse into the conduction band with Nb_{Li}^{5+} centers, as represented by the term $\gamma_X n(N_X - N_X^-)$ in Eq. (6). To make a decisive statement about this process, measurements with higher temporal resolution in the range of a few ps are necessary. Due to the relatively large energetic distance of the polaronic energy levels to the conduction band, we will also neglect thermal excitation of these levels—i.e., $\beta_X=0$. If we chose a sufficiently small probe beam intensity, the main mechanism of polaron decay is a direct transfer of electrons back into empty deep traps, possibly via the formation of small free polarons with shorter lifetimes than the detected small bound polarons, indicated by the term $\gamma_{XY}(N_Y - N_Y^-)N_X^-$ in Eq. (6). However, the fact that $\alpha_{li}(t)$ cannot be described by a single-exponential function but only with a KWW function indicates that γ_{XY} is not constant, a fact that has been reported before.[16] Our measurements show that this stretched exponential decay is not a peculiarity of $LiNbO_3$:Fe, but common to a range of doping elements. The KWW function has been used to describe a large number of different physical processes; it generally is a sign that a system does not have a single well-defined decay time, but rather exhibits a multitude of single-exponential decays with different decay times.[29] As a rule, β decreases with an increasing number of decay times. In this context, the parameter τ obtained from the description of the measured data with Eq. (1) cannot be regarded as *the single* decay time of the system. According to Ref. 30, it can be used to calculate the mean value $\langle\tau\rangle$, corresponding to the integrated area of the normalized $\alpha_{li}(t)$ curve, of this distribution:

$$\langle\tau\rangle = \frac{\tau}{\beta}\Gamma\left[\frac{1}{\beta}\right]. \tag{7}$$

Here, Γ is the gamma function. The actual lifetimes of specific polarons is not necessarily equal to this mean value.

The large number of different decay times indicated by the small values of β has been successfully attributed to the dependence of the lifetime of a polaron to the distance of the nearest empty deep trap.[16] The quantity γ_{XY} decreases with the spatial distance between the polaron and trap, resulting in an increase of the lifetime of a specific polaron. It should be noted that the stretched exponential function fits the measured data very well down to a timescale of several 10^{-9} s if the parameter A_α is left as a free-fitting parameter instead of fixed to the highest value of α_{li} observed in the experiment. A more complex model like the one described in Ref. 27 is therefore not necessary to describe the experimental observations. In contrast, a clear theoretical evaluation of the stretched exponential function is given in Ref. 31 on the basis of a random distribution of trapping sites in a three-dimensional (3D) space, which is in full agreement with our distance-dependent model.[16] No further corrections or parameters are needed. Note that an alternative model can also lead to the stretched exponential behavior. If there exists a distribution of different energy barriers for the polaron decay due to different lattice surroundings in the disordered lattice of congruent $LiNbO_3$, a lot of decay times occur, resulting in the stretched exponential function. This model can be used as a physical basis for the calculations in Ref. 31 and explains the existence of the stretched exponential decay in disordered systems straightforward. But there exists also a distance dependence, shown in Ref. 16, by irradiating the polarons with a second pulse of $\lambda=1064$ nm some ns after the green pulse. The lifetime τ increases drastically. Unfortunately, a clear decision between both models cannot be presented with our results but is under current examination.

The dependence of α_{li} on the polarization direction of pump and probe beams and on the wavelength of the pump beam reflects the differences in the fundamental absorption α of doped $LiNbO_3$: both $q_{YX}s_{YX}$ and q_Xs_X are larger for ordinary light polarization and for lower λ_p. The fact that β shows a slight decrease towards lower λ_p can be explained by the distance-dependent model of decay times or the disordered lattice model: The energetic barrier that has to be crossed to excite electrons from a deep trap into a polaronic state is not necessarily constant, but can depend on several factors such as the distance between the two centers and the surrounding crystal structure. For small λ_p, the increased photon energy can raise the electrons into polaronic states that are not accessible with the low-energy photons at larger pump wavelengths. This increase in the accessible polaronic centers leads to a corresponding increase of the number of different relaxation times in the system, which in turn causes a reduction of the parameter β.

B. Intensity dependence of α_{li}^{max}, τ, and β

It is evident from Eq. (6) that α_{li}^{max} increases with increasing I_p. The absorption $\alpha_{li}^{max}(I_p)$ is described very well with a single-exponential function [Eq. (3)], indicating the validity of a rate equation with only two energetically different levels for the formation of polarons. The Ti-doping ions in LNB:Fe:Ti play only a minor role, which is obvious from the small difference between α_{li}^{max} of LNB:Fe and LNB:Fe:Ti in Fig. 6(a). This observation coincides with the fact that Ti occurs in the form of Ti^{4+} in the crystal: Ti^{4+} ions cannot contribute to polaron formation since they cannot give up a further electron. However, we have to note that the saturation values of α_{li} as well as the slope of $d\alpha_{li}^{max}/dI_0$ for LNB:Fe and LNB:Fe:Ti are equal. Taking the results of Ref. 16 into account, where $d\alpha_{li}^{max}/dI_0$ is determined as a function of $c_{Fe^{2+}}$, $c_{Fe^{3+}}$, and c_{Fe}, the assumption of an increase of $c_{Fe^{2+}}$ in the presence of Ti in our sample is not valid. Both the saturation value of α_{li} and the slope $d\alpha_{li}^{max}/dI_0$ should increase with increasing $c_{Fe^{2+}}$, which contradicts with the results in Fig. 4(a). On the other hand, as it is known that low concen-

trations of Ti (0.04%) do not contribute to the absorption in the relevant spectral range,[26] the concentration $c_{Fe^{2+}}$ determined from the absorption measurements is valid to a sufficient accuracy. In consequence the relation $d\alpha_{li}^{max}/dI_0 = \kappa c$ cannot be used to determine the concentration $c_{Fe^{2+}}$ in double-doped LNB:Fe:Ti, taking κ from the single-doped LNB:Fe. The reason for this might be a decrease of the antisite concentration by introducing the Ti dopants or a pair correlation Fe^{2+}-Ti^{4+} as discussed for Mg^{2+}-Ti^{4+} pairs in LNB:Mg:Ti.[26] Therefore, we have found that every doped material, including double-doped crystals, has its own sensitivity value κ.

The effectiveness of electron excitation from the deep trap is expressed in the parameter κ. While the sensitivity κ of LNB:Fe:Ti is a factor of 2 smaller than that of LNB:Fe, κ of LNB:Cu is a factor of 4 smaller. It has to be noted that even for LNB:Fe, the observed value of κ is by a factor of 4 smaller compared to the values reported in Refs. 16 and 32. Here, it is noteworthy that we used significantly shorter exciting pulses than the ones reported in Ref. 16 beside slightly longer probing wavelengths. Since in both cases the pulse duration was shorter than the lifetime of the polarons, one has to consider the total number of photons, which is proportional to the pump pulse energy E_p. To compare measurements with different pulse durations, one has to look at the slope of $\alpha_{li}^{max}(E_p)$, not $\alpha_{li}^{max}(I_p)$. We therefore observed values of the derivative $d\alpha_{li}^{max}/dI_0$ that are lower by the same factor that our pulse duration is shorter compared to the measurements presented in Ref. 16.

The values of α_{li}^{max} for LNB:Fe and LNB:Fe:Ti show that the generated concentration of polarons is nearly identical in both samples. Apparently, the incorporation of Ti^{4+} influences the absorption spectra significantly by enhancing $c_{Fe^{2+}}$, but reduces the number density of the optically generated polarons. The difference in κ is an indication that the electrons from the deep Fe^{2+} traps are excited in the same way to form $Nb_{Li}{}^{4+}$ polarons, but with a lower concentration in LNB:Fe:Ti due to the presence of Ti, as discussed above. The lowest value of κ is obtained for LNB:Cu, showing that Cu doping is the least sensitive for the excitation of polarons.

The fact that a saturation of $\alpha_{li}^{max}(I_0)$ is actually observed for LNB:Fe and LNB:Fe:Ti shows that a significant number of the deep traps are emptied at pulse intensities of $I_p = 450\ MW/cm^2$. The high absorption of LNB:Cu prevented us from reaching high enough effective intensities in this sample. We can exclude the fact that all available Nb_{Li} centers are filled, because their concentration of $c_{Nb_{Li}} = 6 \times 10^{26}\ m^{-3}$ far exceeds the concentration of any of our doping ions. The increase of the values of β and τ can be explained by taking into account that electrons are not necessarily excited into the polaronic ground state by the pulse. If the wavelength is short enough, so-called "hot" polarons with energies far above the thermal energy of the system can be created. To thermalize, the polarons have to dissipate their energy to the crystal lattice by the creation of phonons by moving through the crystal. For low pump intensities, a few electrons will be excited from their deep traps, preferably to polaronic centers very close to their original position. They will then move through the crystal, some coming to rest close to the then-empty deep centers into which they can decay quickly. Some, however, will reach positions far away from an accessible deep center. These polarons have very long decay times. The resulting broad distribution of decay times leads to small values of β. If the pump intensity is increased, more and more hot polarons are created. The relocation of the polarons leads to a homogenization of their distribution. The mean distance between polaron and deep center grows, leading to an increase of the mean decay time τ, but the deviation of the actual distance from the mean distance decreases, leading to an increase of the stretching parameter β. It has to be noted that τ is significantly smaller in LNB:Fe:Ti than in LNB:Fe. This shows that the Ti^{4+} ions, which cannot take part in the polaron buildup as described above, act as traps for the decay of electrons from their polaronic states, forming an intermediate Ti^{3+} state. The increased number of deep traps results in a reduced lifetime of the polarons.

C. Wavelength dependence of α_{li}^{max}

The fact that $\alpha_{li}^{max}(\lambda_s)$ can be described very well with Eq. (4) in the entire wavelength range is a clear sign for the generation of the small bound $Nb_{Li}{}^{4+}$ polaron. This behavior is very well known and in excellent agreement with previous results.[14,16] The stabilization energy U is slightly reduced in LNB:Fe:Ti but the transfer energy ε increases significantly in this crystal. The maximum of $\alpha_{li}^{max}(\lambda)$ is slightly shifted to larger wavelengths with respect to Ref. 17, a fact that can be explained by the difference of the measurement temperatures: The values reported in Ref. 17 were obtained at 100 K, compared to our room-temperature measurements. Apparently, the transition energy for polarons decreases with increasing temperature. The reduction of U by about 0.05 eV and the increase of ε by about 0.2 eV in LNB:Fe:Ti shows the special role of the double-doped crystal in comparison with the single-doped crystals. It appears that Ti changes these two energies. However, we have to take into account that we had to fix the phonon frequency at 0.1 eV to fit the data with Eq. (4). This certainly has an influence on the obtained values for U and ε.

For technical applications like nonvolatile holographic recording by two-color holography, it is important to know the spectral range in which writing of holograms can be performed. The wavelength dependence of α_{li} shows that even at $\lambda = 1.5\ \mu m$ sufficent α_{li} is present in LNB:Cu for nonvolatile recording.

D. Temperature dependence and activation energy

The increase of α_{li}^{max}—i.e., the increase in the number of polarons generated with a single pulse—with increasing temperature can be understood by keeping in mind that polarons are a combination of electrons and phonons with a characteristic transport behavior. The excited electrons are influenced by their thermal energies via k_BT due to their mobility and transport behavior. For the most likely case that much of the transport between $Nb_{Li}{}^{4+}$ and Fe^{3+} or Cu^{2+} occurs via free small polarons this corresponds to an increase of the mobility

of the conduction band polarons with rising temperature. Consequently, more polarons are created at a given pump wavelength and pulse intensity, and the light-induced absorption increases.

The decay times τ resulting from fits of the KWW function to $\alpha_{\mathrm{li}}(t)$ at different temperatures follow Arrhenius' law. This is a bit surprising at first, since τ represents a large variety of different decay times. Apparently, the collective behavior of this ensemble of decay times is comparable to that of a single physical process, a fact that has been noted before.[16] The obtained values of E_A and Z have physical meanings only as mean values for a large number of single processes. E_A and Z are identical for all experimental conditions. One can thus securely say that $\alpha_{\mathrm{li}}(785\ \mathrm{nm})$ and $\alpha_{\mathrm{li}}(1064\ \mathrm{nm})$ are caused by the same type of polarons for both samples. The polarons are stabilized on their $\mathrm{Nb_{Li}}^{4+}$ lattice sites, regardless of their origin from Fe^{2+} or Cu^{+} deep centers. Neither the energy required to break up the polarons and transport the electrons back to a free deep center nor the attempt frequency with which the electron tries to escape its polaronic well therefore depends on the doping type. The increase of the stretching exponent β with increasing temperature results from a reduction of the width of the decay time distribution: The decay times decrease exponentially with increasing temperature. At very low temperatures, a given distribution of activation energies results in a broad decay-time distribution which becomes narrower as T increases. In the limit of very high temperatures, the decay times become almost independent of the activation energies, $\alpha_{\mathrm{li}}(t)$ can be described by a single-exponential function, and β approaches unity, which is the case at $T=200\ ^{\circ}\mathrm{C}$. Comparing the value of the activation energy E_A from our study with that published in Ref. 16, it is evident that the latter is smaller by about a factor of 2. Inspecting Fig. 8 in Ref. 16 in more detail, one notices a kink in the curve at about 280 K, indicating that the data may have to be explained with two different activation energies, one for the high-temperature part above 280 K and one for the low-temperature part below 280 K. Our study provides an extension to the high-temperature range, as we have measured from 293 K to 473 K. The activation energies of LNB:Fe are determined to 0.39 eV and 0.36 eV for this high-temperature range. Under this aspect we have refitted the data from Fig. 8 in Ref. 16 and obtain $E_A=0.33$ eV for the high-temperature range above 293 K and $E_A=0.14$ eV for the low-temperature range below 280 K. The intersection of the two lines is at $T=281$ K. Therefore, there are two temperature regions exhibiting different activation energies for the small bound polarons. Possibly, this points to a hopping process of the polarons above $T=281$ K, while below this temperature the polarons are at rest. For a more detailed interpretation of this result, further measurements have to be carried out, especially towards lower temperatures.

V. SUMMARY AND CONCLUSIONS

It has been shown that the light-induced absorption in doped $LiNbO_3$ single crystals upon exposure to intense laser light at $\lambda_p=532$ nm can be traced to the excitation of small bound $\mathrm{Nb_{Li}}^{4+}$ polarons for different doping elements. The polarons in doped congruently grown $LiNbO_3$ decay on the time scale of a few μs at room temperature. The fact that the decay is described very well with a stretched exponential function indicates that the observed behavior is a superposition of single decay events with a multitude of different decay times. Due to these results, an earlier model that connects the lifetime of a small polaron to its distance to the nearest free deep trap could be extended to smaller time scales and different types of doping. However, this observed stretched exponential decay behavior might also be explained by the disorder of LNB. From the dependence of the amplitude of the light-induced absorption change on the pump pulse intensity, one could observe that the generation of polarons is more effective for Fe-doped samples than for Cu-doped samples. Codoping with titanium introduces another deep trap into the system, leading to a reduction of the polaron lifetimes. For LNB:Fe and LNB:Cu, the dependence of the light-induced absorption on the probing wavelength can be perfectly explained by the presence of small $\mathrm{Nb_{Li}}^{4+}$ polarons. Temperature-dependent measurements showed an Arrhenius behavior of the polaron decay. The activation energy and the frequency factor are independent of the doping concentration and the probing wavelength, an indication that the behavior of the polarons is dictated merely by the environment of the Nb^{4+} lattice site. Small free polarons, exhibiting an absorption band at about 1 μm, could not be detected in the investigated doped $LiNbO_3$ crystals. The wavelength dependence of the absorption of the small bound polarons shows that two-step recording for nonvolatile holographic data storage might be possible even at 1.5 μm in LNB:Cu.

ACKNOWLEDGMENT

This work was supported by the Deutsche Forschungsgemeinschaft (DFG) within the Project Nos. SPP1056, WO618/3-4, and IM 37/2-1.

[1] F. S. Chen, J. T. LaMacchia, and D. B. Fraser, Appl. Phys. Lett. **13**, 223 (1968).
[2] D. L. Staebler, W. J. Burke, W. Phillips, and J. J. Amodei, Appl. Phys. Lett. **26**, 182 (1975).
[3] X. An, D. Psaltis, and G. W. Burr, Appl. Opt. **38**, 386 (1999).
[4] *Holographic Data Strorage*, edited by H. J. Coufal, D. Psaltis, and G. T. Sincerbox, Springer Series in Optical Sciences (Springer-Verlag, Berlin, 2000).
[5] D. L. Staebler and J. J. Amodei, Ferroelectrics **3**, 107 (1972).
[6] V. V. Kulikov and S. I. Stepanov, Sov. Phys. Solid State **21**, 1849 (1979).
[7] K. Buse, S. Breer, K. Peithmann, S. Kapphan, M. Gao, and E.

Krätzig, Phys. Rev. B **56**, 1225 (1997).
[8] K. Buse, F. Jermann, and E. Krätzig, Ferroelectrics **141**, 197 (1993).
[9] E. M. de Miguel-Sanz, M. Carrascosa, and L. Arizmendi, Phys. Rev. B **65**, 165101 (2002).
[10] H. Guenther, R. MacFarlane, Y. Furukawa, K. Kitamura, and R. Neurgaonkar, Appl. Opt. **37**, 7611 (1998).
[11] I. Nee, M. Müller, K. Buse, and E. Krätzig, J. Appl. Phys. **88**, 4282 (2000).
[12] H. Kurz, E. Krätzig, W. Keune, H. Engelmann, U. Gonser, B. Dischler, and A. Räuber, Appl. Phys. (Berlin) **12**, 355 (1977).
[13] E. Krätzig and R. Orlowski, Ferroelectrics **27**, 241 (1980).
[14] J. Jermann and J. Otten, J. Opt. Soc. Am. B **10**, 2085 (1993).
[15] A. Adibi, K. Buse, and D. Psaltis, Phys. Rev. A **63**, 023813 (2001).
[16] D. Berben, K. Buse, S. Wevering, P. Herth, M. Imlau, and Th. Woike, J. Appl. Phys. **87**, 1034 (2000).
[17] O. F. Schirmer, O. Thiemann, and M. Wöhlecke, J. Phys. Chem. Solids **52**, 185 (1991).
[18] V. Yu. Yakovlev, E. V. Kabanova, T. Weber, and P. Paufler, Phys. Status Solidi A **185**, 423 (2001).
[19] V. Pankratov, D. Millers, L. Grigorjeva, A. O. Matkovskii, P. Potera, I. Prackta, and T. Lukasiewicz, Opt. Mater. (Amsterdam, Neth.) **22**, 257 (2003).
[20] L. Arizmendi, J. M. Cabrera, and F. Agullo-Lopez, J. Phys. C **17**, 515 (1984).
[21] M. G. Clark, F. J. DiSalvo, A. M. Glass, and G. E. Peterson, J. Chem. Phys. **59**, 6209 (1973).
[22] O. Thiemann, H. Donnerberg, M. Wöhlecke, and O. F. Schirmer, Phys. Rev. B **49**, 5845 (1994).
[23] G. Corradi, M. Meyer, L. Kovacs, and K. Polgar, Appl. Phys. B: Lasers Opt. **78**, 607 (2004).
[24] J. Imbrock, A. Wirp, D. Kip, and E. Krätzig, J. Opt. Soc. Am. B **19**, 1822 (2002).
[25] V. Gericke, P. Hertel, E. Krätzig, J. P. Nisius, and R. Sommerfeldt, Appl. Phys. B: Photophys. Laser Chem. **44**, 155 (1987).
[26] J. Liu, W. Zhang, and G. Zhang, Phys. Lett. A **212**, 275 (1996).
[27] De-Long Zhang and E. Y. B. Pun, J. Appl. Phys. **95**, 3437 (2004).
[28] I. G. Austin and N. F. Mott, Adv. Phys. **18**, 41 (1969).
[29] R. V. Chamberlin, Phase Transitions **65**, 169 (1998).
[30] F. Alvarez, A. Alegria, and J. Colmenero, Phys. Rev. B **44**, 7306 (1991).
[31] B. Sturman, E. Podivilov, and M. Gorkunov, Phys. Rev. Lett. **91**, 176602 (2003).
[32] M. Simon, F. Jermann, and E. Krätzig, Opt. Mater. (Amsterdam, Neth.) **3**, 243 (1994).